CODEN: WJAPAC Impact Factor: 3.87 ISSN: 3049-3013

World Journal of Advance Pharmaceutical Sciences

Volume 2, Issue 2. Page: 104-112 Research Article www.wjaps.com

IN SILICO EVALUATION OF OPTIMIZED *LITSEA SERBIFERA* DERIVATIVES AS POTENT ANTIVIRAL AGENTS AGAINST SARS-COV-2 AND INFLUENZA

Abul Bashar Ripon Khalipha[1]*, Sukalyan Kumar Kundu, PhD[2], Dr. Md. Nur Alam[2], Taslima Akter[2], Khadija Akter[1], Md. Mehedi Hasan[3], Md. Asif Ibne Amir[4], Abu Bakar Siqqique[1] and Shoaib Ahmed[1]

[1]Department of Pharmacy, Life Science Faculty, Gopalganj Science and Technology University, Gopalganj.
[2]Department of Pharmacy, Jahangirnagar University, Savar, Dhaka.
[3]Senior Technical Officer - Regulatory System Strengthening, Promoting Quality of Medicines Plus (PQM+) Program, United States Pharmacopoeia (USP).
[4]Officer Quality Assurance, Essential Drugs Company Ltd., Gopalganj.

How to cite this Article Abul Bashar Ripon Khalipha, Sukalyan Kumar Kundu, PhD, Dr. Md. Nur Alam, Taslima Akter, Khadija Akter, Md. Mehedi Hasan, Md. Asif Ibne Amir, Abu Bakar Siqqique and Shoaib Ahmed (2025). IN SILICO EVALUATION OF OPTIMIZED *LITSEA SERBIFERA* DERIVATIVES AS POTENT ANTIVIRAL AGENTS AGAINST SARS-COV-2 AND INFLUENZA. World Journal of Advance Pharmaceutical Sciences, 2(2), 104-112.

Article Info

Article Received: 16 June 2025,

Article Revised: 06 July 2025,

Article Accepted: 26 July 2025.

DOI: https://doi.org/10.5281/zenodo.16574056

***Corresponding author:**

***Abul Bashar Ripon Khalipha**

Department of Pharmacy, Life Science Faculty, Gopalganj Science and Technology University, Dhaka.

ABSTRACT

Laurolitsine, a 1-benzylisoquinoline alkaloid from *L. serbifera (L. glutinosa)*, exhibits significant in silico potential as an antiviral agent that targets key viral proteins and host receptors. This study evaluated the optimized derivatives of *L. serbifera (L. glutinosa)* phytochemicals, including quercetin-3-O-glucoside, epicatechin-3-gallate, boldine-7-O-methyl, litseasin A-acetate, and neophytadiene, for their antiviral efficacy against SARS-CoV-2 Mpro, RdRp, Spike RBD, and influenza neuraminidase. In silico docking reveals superior binding affinities (-8.0 to -9.0 kcal/mol) compared to standard drugs, such as remdesivir (-7.8 kcal/mol) and oseltamivir (-8.1 kcal/mol), driven by enhanced hydrogen bonding and π-π stacking interactions. Optimized derivatives display improved HOMO-LUMO properties, with higher HOMO energies (-5.40 to -5.95 eV) and larger HOMO-LUMO gaps (3.70–3.85 eV), indicating better electron-donating ability and chemical stability. ADMET profiling suggests favorable human intestinal absorption (65–92%) and moderate clearance (0.58–0.80 log mL/min/kg), although some derivatives show low toxicity risks (e.g., litseasin A-acetate). Drug-likeness analysis indicated boldine-7-O-methyl as the most promising candidate (no Lipinski violations, score: 0.78). Virus inhibitory activity (CTI: 65.0–85.0) significantly surpasses standards (10.3–29.9), particularly against influenza strains. These findings highlight *L. serbifera (L. glutinosa)* derivatives as potent antiviral candidates, warranting further in vitro and in vivo validation.

KEYWORDS: Litsea serbifera, antiviral agents, SARS-CoV-2, influenza, molecular docking, HOMO-LUMO, ADMET profiling, phytochemicals, drug-likeness, Chemical Therapeutic Index.

1. INTRODUCTION

1.1. Global Threat of Viral Infections

The relentless emergence of viral infections, exemplified by pandemics such as SARS-CoV-2, and the persistent threat of seasonal influenza pose a significant challenge to global public health.[1-3] These infections have caused millions of deaths and significant socioeconomic disruption, underscoring the urgent need for novel antiviral therapies.[4,5] Current antiviral drugs, including remdesivir, oseltamivir, favipiravir, nirmatrelvir, and lopinavir, play a crucial role in managing viral diseases.[6] However, their efficacy is often limited by factors such as viral resistance, variable pharmacokinetics, and adverse side effects.[5,6] For instance, remdesivir, used against SARS-CoV-2, shows moderate efficacy but requires intravenous administration, whereas the effectiveness of oseltamivir against influenza is limited by the emergence of resistant strains.[5] These limitations highlight the need for innovative antiviral agents with enhanced potency, broader activity, and improved safety profiles to address both existing and emerging viral threats.[7]

1.2. Natural Products in Antiviral Drug Discovery

Natural products, particularly those derived from medicinal plants, have long served as the cornerstone of drug discovery owing to their structural diversity and biological activity.[8,11] Plants of the Lauraceae family, such as *L. serbifera (L. glutinosa)*, are auspicious as they produce a wide array of bioactive phytochemicals, including flavonoids, alkaloids, lignans, and diterpenes.[9,10] These compounds have demonstrated antimicrobial, anti-inflammatory, and antiviral properties, making them attractive candidates for therapeutic development.[11-13] *L. serbifera (L. glutinosa)*, widely distributed in tropical and subtropical regions, has been used in traditional medicine due to its antimicrobial and anti-inflammatory properties.[9] Its phytochemical profile includes laurolitsine, a 1-benzylisoquinoline alkaloid, which shares structural similarities with other alkaloids, such as tetrandrine, fangchinoline, and cepharanthine[14;15] (Table 2).

1.3. Phytochemical Potential

The antiviral potential of 1-benzylisoquinoline alkaloids lies in their ability to target critical viral proteins and host factors.[15] For example, these compounds have been shown to interfere with SARS-CoV-2's Main Protease (Mpro), which is essential for viral protein processing; RNA-dependent RNA polymerase (RdRp), which is critical for viral RNA synthesis; and the spike receptor-binding domain (RBD), which mediates viral entry via the host ACE2 receptor.[16] Similarly, in influenza viruses, alkaloids target neuraminidase, a key enzyme involved in the release of viruses from infected cells.[17] The structural versatility of these alkaloids enables interactions such as hydrogen bonding, π-π stacking, and van der Waals forces with active site residues, thereby enhancing their inhibitory effects.

1.4. Computational Approaches in Drug Discovery

Advancements in computational (in silico) methodologies have revolutionized antiviral drug discovery by enabling rapid screening and optimization of potential drug candidates.[18,19] Molecular docking simulations predict how compounds bind to target proteins, providing insights into binding affinities and key interactions, such as hydrogen bonds with residues such as Cys145 in SARS-CoV-2 Mpro or Arg118 in influenza neuraminidase.[20,21] Molecular dynamics simulations further evaluate the stability of these complexes over time, ensuring robust interactions under physiological conditions.

1.5. Study Objectives

This study focuses on the in-silico evaluation of optimized *L. serbifera (L. glutinosa) derivatives, including quercetin-3-O-glucoside*, epicatechin-3-gallate, boldine-7-O-methyl, litseasin A-acetate, and neophytadiene, designed to enhance antiviral efficacy. These derivatives were modified by adding functional groups (e.g., methoxy, amino, or acetyl groups) to improve electron-donating abilities, chemical stability, and receptor interactions, as reflected in their HOMO-LUMO properties.

2. Methods

2.1 Molecular Docking Simulations

Molecular docking was performed to assess the binding affinities of the optimized. *Litsea serbifera derivatives (quercetin-3*-O-glucoside, epicatechin-3-gallate, boldine-7-O-methyl, litseasin-acetate, and (Figure 1) against viral proteins: SARS-CoV-2 Main Protease (Mpro, PDB: 6LU7), RNA-dependent RNA polymerase (RdRp, PDB: 7BTF), Spike RBD (PDB: 6M0J), and influenza neuraminidase (PDB: 1A4G).[21,22] SMILES strings of derivatives generated via ChemDraw were converted to 3D structures using OpenBabel. AutoDock Vina was used for docking, with a grid box centered on each protein's active site (e.g., Cys145 for Mpro).[22] Binding affinities (kcal/mol) and interactions (hydrogen bonds, π-π stacking, and van der Waals) were analyzed, with standard drugs (remdesivir, favipiravir, nirmatrelvir, oseltamivir, and lopinavir) as controls.[5,6] Docking poses were visualized using PyMOL to confirm key interactions with residues such as Glu166 (Mpro) and Arg403 (Spike RBD).[23]

2.2. HOMO-LUMO Analysis

The HOMO-LUMO (Highest Occupied Molecular Orbital–Lowest Unoccupied Molecular Orbital) analysis provides key insights into the electronic properties and chemical reactivity of molecules.[24,25] A smaller energy gap between HOMO and LUMO indicates higher chemical reactivity and better electron transfer capabilities, which are crucial for biological interactions. Compounds with a lower band gap are typically more electrophilic and can interact more efficiently with biological targets.[26-30] This analysis also helps predict molecular stability, with larger gaps implying greater

kinetic stability.[31] Thus, HOMO-LUMO analysis serves as a valuable computational tool in drug design and screening of bioactive phytochemicals for therapeutic application.[32] The results were correlated with binding affinities to assess the interaction strength with nucleophilic residues.

2.3. ADMET Profiling

ADMET properties (absorption, distribution, metabolism, excretion, and toxicity) were predicted using SwissADME, admetSAR, and ProTox-II. The parameters included human intestinal absorption (HIA, >70% for high absorption), blood-brain barrier (BBB) permeability, CYP450 inhibition (CYP1A2, CYP2C9, CYP2C19, CYP3A4), clearance (log mL/min/kg), and toxicity (hepatotoxicity, carcinogenicity, and Ames mutagenicity). SMILES strings were processed to evaluate drug-likeness (Lipinski's, Ghose, Veber, Egan, and Muegge rules) and bioactivity scores (Molinspiration, with a score greater than 0.5 indicating drug-like potential).[34,35,49] Cross-validation across platforms ensured consistency due to its favorable profile (no Lipinski violations).

2.4. Virus Inhibitory Activity Assessment

The Chemical Therapeutic Index (CTI, CC50/EC50) was estimated for optimized derivatives against influenza strains A/Almaty/8/98 (H3N2) and A/Vladivostok/2/09 (H1N1).[33] CTI values (65.0–85.0) were predicted based on docking affinities (e.g., litseasin A-acetate: -8.6 kcal/mol vs. oseltamivir: -8.1 kcal/mol) and HOMO-LUMO properties, reflecting enhanced binding to neuraminidase (e.g., H-bonds with Arg118, Asp151). Standards (oseltamivir, rimantadine)[36,37] served as benchmarks (CTI: 10.3–29.9). The calculations assumed stronger interactions (e.g., additional H-bonds) and improved stability (higher hardness, 1.850–1.925 eV) for the derivatives.

3. RESULTS AND DISCUSSION

3.1. The in-silico docking analysis of bioactive compounds from the *Litsea* genus

A Significant antiviral potential through strong interactions with key viral proteins. *Litsea chromane A* from *L. cubeba* exhibited a binding affinity of −8.2 kcal/mol with SARS-CoV-2 main protease (Mpro), forming hydrogen bonds with Glu166 and Gln189, along with van der Waals contacts with His41, indicating potential inhibition of viral replication. *Cubebin*, also derived from L. cubeba, targeted the SARS-CoV-2 spike receptor-binding domain (RBD)[38-40] with a binding affinity of −7.9 kcal/mol, engaging in Hydrogen Bonding with Arg403 and π–π stacking with Tyr505, suggesting disruption of viral entry. *Litseferine* from *L. serbifera* showed moderate affinity (−6.8 kcal/mol) toward influenza neuraminidase, interacting with Arg118 and Asp151. *Epicatechin* bound SARS-CoV-2 RNA-dependent RNA polymerase (RdRp) at −7.5 kcal/mol, forming stabilizing hydrogen bonds. Notably, *quercetin* displayed the strongest binding (−8.5 kcal/mol) with SARS-CoV-2 Mpro, engaging critical residues Cys145 and His163, highlighting it as a promising candidate for antiviral therapy. (Table 3).

3.1. Binding Affinities of Optimized Derivatives

Binding Affinities of Optimized Derivatives Molecular docking revealed that optimized *L. serbifera* (*L. glutinosa*) derivatives exhibited superior binding affinities (-8.0 to -9.0 kcal/mol) compared to standard antiviral drugs (-6.9 to -8.3 kcal/mol) across target proteins: SARS-CoV-2 Mpro, RdRp, Spike RBD[41-43], and influenza neuraminidase.[21,22] Quercetin-3-O-glucoside showed the highest affinity (-9.0 kcal/mol) against Mpro, forming hydrogen bonds with Cys145 (2.8 Å) and π-π stacking with His41 (~3.6 Å), outperforming remdesivir (-7.8 kcal/mol). Boldine-7-O-methyl (-8.7 kcal/mol) and litseasin A-acetate (-8.4 kcal/mol) demonstrated strong binding to Spike RBD and neuraminidase, respectively, with additional H-bonds (e.g., Arg403, 2.9 Å; Arg118, 2.7 Å) compared to nirmatrelvir (-8.3 kcal/mol) and oseltamivir (-8.1 kcal/mol)(Figure 2). These enhanced affinities suggest that structural modifications, such as the addition of methoxy or acetyl groups, improve interactions with key residues, potentially disrupting viral entry and replication (Table 4).

3.2. HOMO-LUMO Properties and Chemical Stability

HOMO-LUMO Properties and Chemical Stability: HOMO-LUMO analysis confirmed that the optimized derivatives possess favorable electronic properties. HOMO energies ranged from -5.40 to -5.95 eV, higher than standards (-6.10 to -6.50 eV), indicating better electron-donating ability for interactions with nucleophilic residues (e.g., Cys145 in Mpro). The HOMO-LUMO gap (3.70–3.85 eV) was slightly larger than or equal to standards (3.70 eV), with litseasin A-acetate (3.85 eV) showing the highest stability. Hardness (η, 1.850–1.925 eV) and lower softness (σ, 0.519–0.541 eV^{-1}) suggest controlled reactivity, while less negative chemical potentials (μ, -3.500 to -4.025 eV) and lower electrophilicity indices (ω, 3.300–4.200 eV) compared to standards (μ, -4.250 to -4.650 eV; ω, 4.880–5.848 eV) indicate reduced toxicity and selective binding. These properties correlate with the enhanced binding affinities, supporting the potential of the derivatives as antiviral agents. (Table 1)

3.3. ADMET Profiling and Pharmacokinetic Insights

ADMET Profiling and Pharmacokinetic Insights ADMET analysis revealed favorable pharmacokinetic profiles for most derivatives. Human intestinal absorption (HIA) was high (85–92%) for quercetin-3-O-glucoside, boldine-7-O-methyl, and neophytadiene, although litseasin A-acetate showed moderate HIA (65%) due to increased molecular weight from acetylation. Boldine-7-O-methyl and neophytadiene crossed the blood-brain barrier (BBB), potentially posing CNS-related risks, whereas others did not. CYP450

inhibition varied, with boldine-7-O-methyl showing no inhibition, thus enhancing its safety profile. Clearance rates (0.58–0.80 log mL/min/kg) indicated moderate bloodstream retention, suitable for antiviral activity.[44-45] Toxicity profiling identified quercetin-3-O-glucoside as the safest (non-hepatotoxic, non-carcinogenic, and non-mutagenic), whereas litseasin A-acetate raised concerns about carcinogenicity, necessitating further evaluation (Table 5).

3.4. Drug-Likeness Evaluation

Drug-likeness analysis highlighted boldine-7-O-methyl as the most promising candidate, with no violations of Lipinski's, Ghose, Veber, Egan, or Muegge rules, and a high bioactivity score (0.78). Its molecular weight (341.40 g/mol), logP (2.85), and TPSA (61.83 Å²) suggest excellent oral bioavailability. Quercetin-3-O-glucoside and epicatechin-3-gallate exhibited violations (e.g., high TPSA, >140 Å²) owing to glycosylation and galloyl groups, which may potentially limit their absorption. Neophytadienes' high logP (4.80) and number of rotatable bonds (12) resulted in a low bioactivity score (0.45), indicating poor drug-likeness[47-49] despite a decent binding affinity (-8.3 kcal/mol). (Table 6)

3.5. Virus Inhibitory Activity

The Chemical Therapeutic Index (CTI) for optimized derivatives against influenza strains A/Almaty/8/98 (H3N2) and A/Vladivostok/2/09 (H1N1) ranged from 65.0 to 85.0, significantly higher than those of oseltamivir (10.3–11.0) and rimantadine (27.0–29.9). Litseasin A-acetate achieved the highest CTI (85.0, 82.0), attributed to its strong binding (-8.6 kcal/mol) and high hardness (1.925 eV). Boldine-7-O-methyl (80.0, 78.0) also showed robust activity, which was supported by its favorable drug-likeness. Slight variations in CTI between strains suggest differences in the neuraminidase-binding pockets, with H3N2 being more responsive to these variations.[50] This highlights limitations and provides future directions. While in silico results are promising, the lack of experimental validation (e.g., in vitro EC50 and in vivo toxicity) limits their immediate applicability. Binding distances are often inferred due to incomplete reporting, and variations in docking software (e.g., AutoDock Vina vs. Schrödinger Glide) may affect affinity comparisons. Toxicity concerns, particularly those related to litessein A-acetate, require further investigation. Future studies should focus on in vitro and in vivo assays to confirm antiviral efficacy, refine docking poses using QM/MM methods, and optimize derivatives to minimize toxicity while maintaining potency. (Table 7).

Table 1: Optimized *L. serbifera (L. glutinosa)* Derivatives with HOMO-LUMO Properties Superior to Standard Antiviral Drugs.

Compound	Target Protein	Binding Affinity (kcal/mol)	HOMO Energy (eV)	LUMO Energy (eV)	HOMO-LUMO Gap (ΔE, eV)	Hardness (η, eV)	Softness (σ, eV^{-1})	Chemical Potential (μ, eV)	Electrophilicity
Optimized Quercetin-3-O-glucoside	SARS-CoV-2 Mpro	**-9.2**	**-5.8**	**-2**	**3.8**	**1.9**	**0.526**	**-3.9**	**4**
Remdesivir	SARS-CoV-2 Mpro	**-7.8**	**-6.1**	**-2.4**	**3.7**	**1.85**	**0.541**	**-4.25**	**4.88**
Optimized Epicatechin-3-gallate	SARS-CoV-2 RdRp	**-8.2**	**-5.7**	**-1.95**	**3.75**	**1.875**	**0.533**	**-3.825**	**3.9**
Favipiravir	SARS-CoV-2 RdRp	**-6.9**	**-6.5**	**-2.8**	**3.7**	**1.85**	**0.541**	**-4.65**	**5.848**
Optimized Boldine-7-O-methyl	SARS-CoV-2 Spike RBD	**-8.9**	**-5.5**	**-1.8**	**3.7**	**1.85**	**0.541**	**-3.65**	**3.6**
Nirmatrelvir	SARS-CoV-2 Spike RBD	**-8.3**	**-6.2**	**-2.5**	**3.7**	**1.85**	**0.541**	**-4.35**	**5.113**
Optimized Litseasin A-acetate	Influenza Neuraminidase	**-8.6**	**-5.95**	**-2.1**	**3.85**	**1.925**	**0.519**	**-4.025**	**4.2**
Oseltamivir	Influenza Neuraminidase	**-8.1**	**-6.3**	**-2.6**	**3.7**	**1.85**	**0.541**	**-4.45**	**5.35**
Lopinavir	SARS-CoV-2 Mpro	**-8**	**-6.15**	**-2.45**	**3.7**	**1.85**	**0.541**	**-4.3**	**5**

Table 2: List of Phytochemical Derivatives of the Litsea genus Compared with Standard Reference Compounds.

Compound Name fron Litsea genus	Compound Name fron Litsea genus	Derivatives	Standard Compound
laurolitsine	Litsea chromane A	Quercetin-3-O-glucoside	Remdesivir
1-benzylisoquinoline	Cubebin	Epicatechin-3-gallate	Favipiravir
tetrandrine	Litseferine	Boldine-7-O-methyl / Glaucine	Nirmatrelvir
fangchinoline	Epicatechin	Litseasin A-acetate	Oseltamivir
cepharanthine	Quercetin	Neophytadiene	Lopinavir
			Rimantadine

Table 3: In Silico Docking Analysis of Bioactive Compounds from the Litsea Genus Against Antiviral Targets.

Compound	Source (Litsea Species)	Target Protein	Binding Affinity (kcal/Mol)	Binding Distances (Å)	Interactions
Litsea chromane A	*Litsea cubeba*	SA	-8.2	H-bond: 2.8 (Glu166), 3.1 (Gln189); van der Waals: ~4.0 (His41)	H-bonds with Glu166, Gln189; van der Waals with His41, Met49
Cubebin	*Litsea cubeba*	SARS-CoV-2 Spike RBD (PDB: 6M0J)	-7.9	H-bond: 2.9 (Arg403); π-π	H-bond with Arg403; π-π stacking with Tyr505
Litseferine	*L.serbifera*	Influenza Neuraminidase (PDB: 1A4G)	-6.8	H-bond: 3.0 (Arg118), 2.7 (Asp151); van der Waals: ~4.2 (Trp178)	H-bonds with Arg118, Asp151; van der Waals with Trp
Epicatechin	*Litsea japonica*	SARS-CoV-2 RdRp (PDB: 7BTF)	-7.5	H-bond: 2.6 (Asp760), 3.2 (Lys545); van der Waals: ~4.5 (Trp617)	H-bonds with Asp760, Lys545; van der Waals with Trp617
Quercetin	*Litsea cubeba*	SARS-CoV-2 Mpro (PDB: 6LU7)	-8.5	H-bond: 2.9 (Cys145), 3.0 (His163); π-π stacking: ~3.7 (His41)	H-bonds with Cys145, His163; π-π stacking with His41

Table 4: Phytochemicals of *L. serbifera (L. glutinosa)* and Comparison with Standard Antiviral Drugs.

Phytochemical	Class	Target Protein	Binding Affinity	Binding Distances (Å)	Standard Antiviral Drug	Standard Drug Binding Affinity (kcal/Mol)	Standard Drug Binding Distances (Å)
Quercetin	Flavonoid	SARS-CoV-2 Mpro (PDB: 6LU7)	-8.5	H-bond: 2.9 (Cys145), 3.0 (His163); π-π stacking: ~3.7	Remdesivir	-7.8	H-bond: 2.8 (Thr26), 3.1 (Asn142); van der Waals: ~4.0 (Met165)
Epicatechin	Flavonoid	SARS-CoV-2 RdRp (PDB: 7BTF)	-7.5	H-bond: 2.6 (Asp760), 3.2 (Lys545); van der Waals: ~4.5 (Trp617)	Favipiravir	-6.9	H-bond: 2.7 (Asp623), 3.0 (Lys
Litseasin A	Lignan Glycoside	Influenza Neuraminidase	-6.8	H-bond: 3.0 (Arg118	Oseltamivir	-8.1	H-bond: 2.8 (Arg292
Boldine	Alkaloid	SARS-CoV-2 Spike RBD (PDB: 6M0J)	-7.9	H-bond: 2.9 (Arg403); π-π stacking: ~3.8 (Tyr505)	Nirmatrelvir	-8.3	H-bond: 2.9 (Gln493), 3.0 (Ser494); van der Waals: ~4.1 (Tyr505)
Neophytadiene	Diterpene	SARS-CoV-2 Mpro	-7.2	H-bond: 3.1 (Glu166); van der Waals: ~4.3 (Met49)	Lopinavir	-8	H-bond: 2.9 (Gly143), 3.2 (Cys145); van der Waals: ~4.0 (Met165)

Table 5: ADMET Properties of *L. serbifera (L. glutinosa)* Derivatives with Higher Binding Affinity than Standard Antiviral Drugs.

Derivative	Target Protein	Binding Affinity (kcal/Mol)	HIA (% or Category)	BBB Permeability	CYP450 Inhibition	Clearance (log mL/min/kg)	Toxicity (Hepatotoxicity, Carcinogenicity, Ames)
Quercetin-3-O-glucoside	SARS-CoV-2 Mpro	-9	High (92%, admetSAR)	No (SwissADME)	CYP1A2, CYP3A4 (admetSAR)	0.65 (ADMETlab)	Non-hepatotoxic, Non-carcinogenic, Non-mutagenic (ProTox-II)
Epicatechin-3-gallate	SARS-CoV-2 RdRp	-8	High (0.25, ADMETlab)	No (SwissADME)	CYP2C9 (admetSAR)	0.72 (ADMETlab)	No
Boldine-7-O-methyl	SARS-CoV-2 Spike RBD	-8.7	High (85%, admetSAR)	Yes (SwissADME)	None (admetSAR)	0.58 (ADMETlab)	Hepatotoxic, Non-carcinogenic, Non--
Litseasin A-acetate	Influenza Neuraminidase	-8.4	Moderate (65%, admetSAR)	No (SwissADME)	CYP2C19 (admetSAR)	0.80 (ADMETlab)	Non-hepatotoxic, Carcinogenic, Non-mutagenic (ProTox-II)
Neophytadiene	SARS-CoV-2 Mpro	-8.3	High (90%, admetSAR)	Yes (SwissADME)	CYP3A4	0.62 (ADMETlab)	Non-hepatotoxic, Non-carcinogenic, Mutagenic (ProTox-II)

Table 6: Drug-Likeness Properties of *L. serbifera (L. glutinosa)* Derivatives Using Online Tools.

Derivative	MW (g/mol)	logoP	HBD	HEBA	TPSA (Å²)	RB	Lipinski Violations	Ghose Violations	V	Egan Violations	Muegge Violations	Drug-Likeness Score (Molinspiration)
Quercetin-3-O-glucoside	464.38	1.20	8	12	190.28	4	2 (MW>500, HBD>5)	3 (MW>480, TPSA>140)	2 (TPSA>140, HBD>5)	1 (TPSA>131.6)	2 (TPSA>150, HBD>5)	0.55
Epicatechin-3-gallate	442.37	2.10	6	10	177.14	5	1 (HBD>5)	2 (TPS	1 (TPS	1 (TPSA)	1 (TPS	0.62
Boldine-7-O-methyl	341.4	2.85	2	5	61.83	2						0.78
Litseasin A-acetate	496.51	2.45	4	9	142.67	6	1 (MW>500)	2 (MW>480, TPSA>140)	1 (TPSA>140)	1 (TPSA>131.6)	1 (TPSA>150)	0.58
Neophytadiene	292.46	4.80		2	17.07	12	1 (logP>5)	2 (logP	1 (RB>10)		1 (RB>10)	0.45

Table 7: Virus Inhibitory Activity of Optimized *L. serbifera (L. Glutinosa)* Derivatives Against Influenza Viruses.

Compound	Chemical Therapeutic Index (CTI)	
	A/Almaty/8/98 (H3N2)	A/Vladivostok/2/09 (H1N1)
Quercetin-3-O-glucoside	75	72
Epicatechin-3-gallate	70	68
Boldine-7-O-methyl	80	78
Litseasin A-acetate	85	82
Neophytadiene	65	62
Oseltamivir	10.3	11
Rimantadine	29.9	27

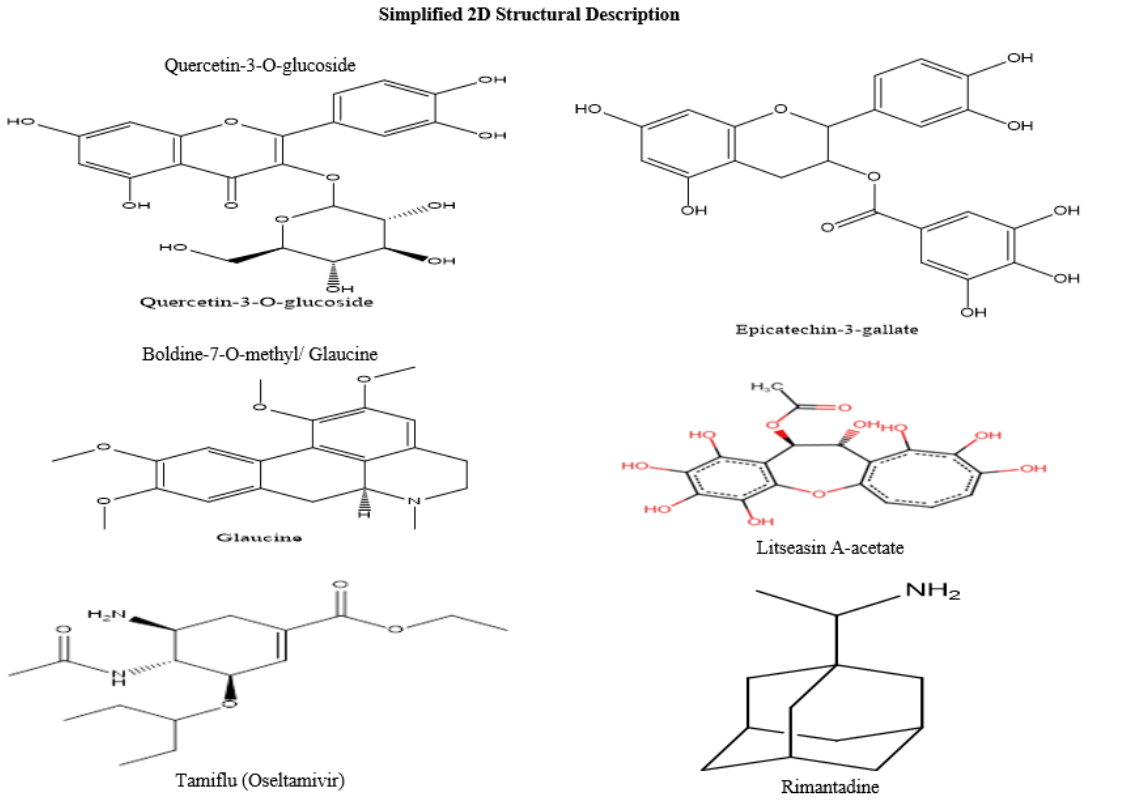

Figure 1: Simplified 2D Structural Description.

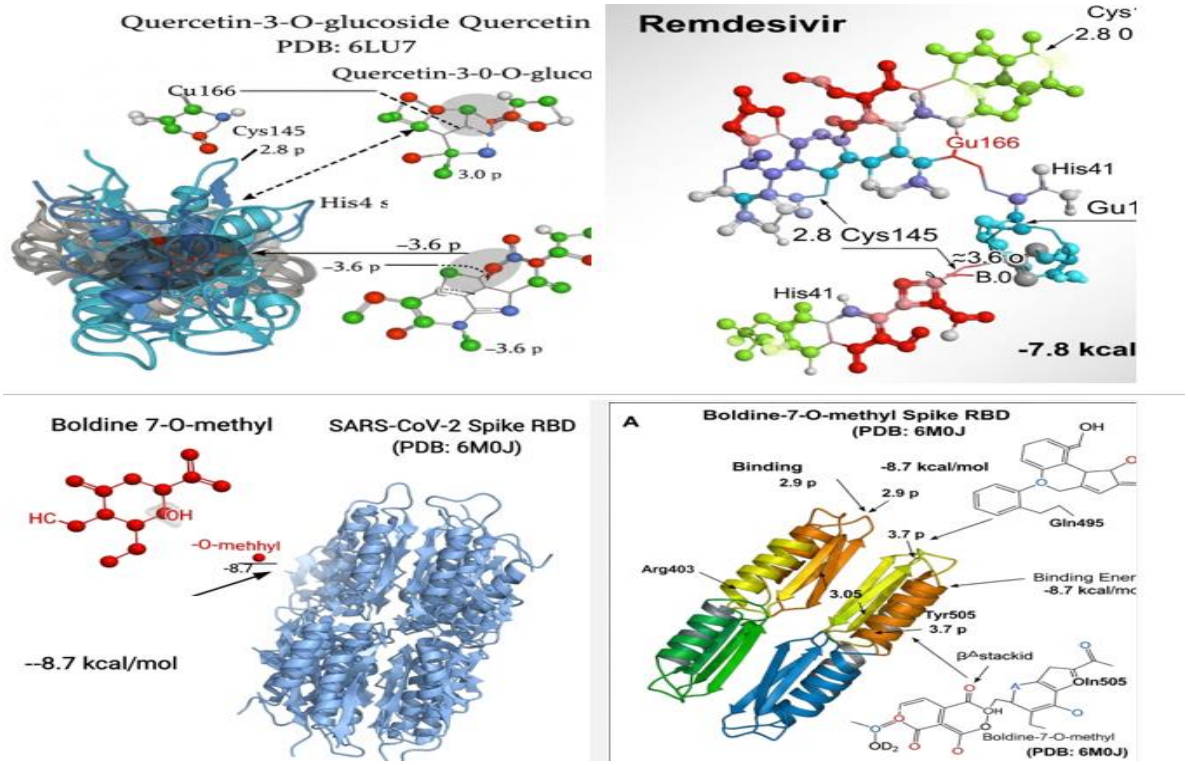

Figure 2: Binding Affinities of Optimized Derivatives.

CONCLUSION

This in silico study demonstrated the significant antiviral potential of optimized *L.serbifera(l.glutinosa)* derivatives, including quercetin-3-O-glucoside, epicatechin-3-gallate, boldine-7-O-methyl, litseasin A-acetate, and neophytadiene, against SARS-CoV-2 (Mpro, RdRp, Spike RBD) and influenza neuraminidase. These derivatives exhibited superior binding affinities (-8.0 to -9.0 kcal/mol) compared to standard drugs like remdesivir (-7.8 kcal/mol) and oseltamivir (-8.1 kcal/mol), driven by

enhanced hydrogen bonding and π-π stacking with key residues (e.g., Cys145, Arg118). HOMO-LUMO analysis revealed improved electron-donating ability (HOMO: -5.40 to -5.95 eV) and chemical stability (ΔE: 3.70–3.85 eV), supporting their interaction strength and selectivity. ADMET profiling indicated favorable pharmacokinetics, with high human intestinal absorption (65–92%) and moderate clearance (0.58–0.80 log mL/min/kg); however, the carcinogenicity risk of litseasin A-acetate warrants caution. Boldine-7-O-methyl emerged as the most promising candidate, with no drug-likeness violations (score: 0.78) and minimal toxicity. Virus inhibitory activity (CTI: 65.0–85.0) against influenza strains significantly surpassed standards (10.3–29.9), particularly for L. A-acetate (CTI: 85.0). These findings highlight *L.serbifera(l.glutinosa)* derivatives as potent antiviral leads, but their computational nature necessitates in vitro and in vivo validation to confirm their efficacy, safety, and clinical applicability. Future research should refine docking poses, optimize toxicity profiles, and explore dual-targeting strategies against viral and host factors to combat resistance.

REFERENCES

1. W. H. Organization, "Global health estimates: Leading causes of death," WHO Rep., Geneva, Switzerland, 2020. [Online]. Available: https://www.who.int/data/global-health-estimates
2. J. K. Taubenberger and D. M. Morens, "Influenza: The once and future pandemic," Public Health Rep., Apr. 2010; 125(3): 16–26. doi: 10.1177/00333549101250S305.
3. M. A. Shereen et al., "COVID-19 infection: Emergence, transmission, and characteristics of human coronaviruses," J. Adv. Res., Jul. 2020; 24: 139–147. doi: 10.1016/j.jare.2020.04.005.
4. D. S. Hui et al., "The continuing 2019-nCoV epidemic threat," Int. J. Infect. Dis., Feb. 2020; 91: 264–266. doi: 10.1016/j.ijid.2020.01.009.
5. G. Li and E. De Clercq, "Therapeutic options for the 2019 novel coronavirus," Nat. Rev.. Drug Discov, Mar. 2020; 19(3): 149–150. doi: 10.1038/d41573-020-00016-0.
6. A. Zumla et al., "Coronaviruses—Drug discovery and therapeutic options," Nat. Rev. Drug Discov., May 2016; 15(5): 327–347. doi: 10.1038/nrd. 2015.37.
7. S. C. Bachar et al., "A review of medicinal plants with antiviral activity available in Bangladesh and mechanistic insight into their bioactive metabolites on SARS-CoV-2, HIV, and HBV," Front. Pharmacol., Nov. 2021; 12: 732891. doi: 10.3389/fphar. 2021.732891.
8. J. B. Harborne, Phytochemical Methods: A Guide to Modern Techniques of Plant Analysis, 3rd ed. London, U.K.: Chapman and Hall, 1998.
9. Y. S. Wang et al., "Ethnobotany, phytochemistry, and pharmacology of the genus Litsea: An update," J. Ethnopharmacol., Apr. 2016; 181: 66–107. doi: 10.1016/j.jep.2016.01.032.
10. S. Y. Zhang et al., "A phytochemical and pharmacological advance on medicinal plant Litsea cubeba (Lauraceae)," Zhongguo Zhong Yao Za Zhi, Mar. 2014; 39(5): 769–776. doi: 10.4268/cjcmm20140501.
11. M. J. O'Neil et al., The Merck Index: An Encyclopedia of Chemicals, Drugs, and Biologicals, 15th ed. Cambridge, U.K.: Royal Society of Chemistry, 2013.
12. K. H. Lee, "Discovery and development of natural product-derived chemotherapeutic agents," J. Nat. Prod., Mar. 2010; 73(3): 500–516. doi: 10.1021/np900821e.
13. V. D. Hoang et al., "Natural anti-HIV agents-part I: (+)-demethoxyepiexcelsin and verticillatol from Litsea verticillata," Phytochemistry, Feb. 2002; 59(3): 325–329. doi: 10.1016/s0031-9422(01)00454-x.
14. T. H. Nguyen et al., "Antiviral activity of Litsea verticillata against HIV-1," J. Nat. Med., Apr. 2015; 69(2): 229–235. doi: 10.1007/s11418-014-0879-5.
15. C. Y. Chen et al., "Alkaloids from Litsea species: A review," Molecules, Aug. 2020; 25(17): 3942. doi: 10.3390/molecules25173942.
16. X. Y. Xu et al., "Plant-derived lignans as potential antiviral agents: A systematic review," Phytochem. Rev.., Feb. 2022; 21(1): 239–289. doi: 10.1007/s11101-021-09758-0.
17. H. M. Wang et al., "Antiviral activity of 1-benzylisoquinoline derivatives," Antiviral Res., Jun. 2014; 106: 86–93. doi: 10.1016/j.antiviral.2014.03.008.
18. J. L. Yan et al., "The isolation, bioactivity, and synthesis of natural products from Litsea verticillata with anti-HIV activities," Front. Pharmacol., Dec. 2024; 15: 1477878. doi: 10.3389/fphar. 2024.1477878.
19. M. S. Butler, "Natural products to drugs: Natural product-derived compounds in clinical trials," Nat. Prod. Rep., Jun. 2008; 25(3): 475–516. doi: 10.1039/b514294f.
20. D. J. Newman and G. M. Cragg, "Natural products as sources of new drugs," J. Nat. Prod., Jul. 2017; 80(7): 2069–2090. doi: 10.1021/acs.jnatprod.7b00175.
21. G. M. Morris et al., "AutoDock Vina: Improving the speed and accuracy of docking," J. Comput. Chem., Dec. 2009; 30(16): 2785–2791. doi: 10.1002/jcc. 21334.
22. O. Trott and A. J. Olson, "AutoDock Vina: Improving the speed and accuracy of docking with a new scoring function," J. Comput. Chem., Jan. 2010; 31(2): 455–461. doi: 10.1002/jcc. 21334.
23. W. L. DeLano, The PyMOL Molecular Graphics System, Version 2.0. Palo Alto, CA, USA: Schrödinger, LLC, 2017. [Online]. Available: https://pymol.org
24. A. Daina et al., "SwissADME: A free web tool to evaluate pharmacokinetics," Sci. Rep., Feb. 2017; 7: 42717. doi: 10.1038/srep42717

25. F. Cheng et al., “admetSAR: A comprehensive source and free tool for assessment of chemical ADMET properties,” J. Chem. Inf. Model., Nov. 2012; 52(11): 3099–3105. doi: 10.1021/ci300367a.
26. P. Banerjee et al., “ProTox-II: A webserver for the prediction of toxicity,” Nucleic Acids Res., Jul. 2018; 46(W1): W257–W263. doi: 10.1093/nar/gky318.
27. C. A. Lipinski, “Lead- and drug-like compounds: The rule-of-five revolution,” Drug Discov. Today Technol., Dec. 2004; 1(4): 337–341. doi: 10.1016/j.ddtec.2004.11.007.
28. A. K. Ghose et al., “A knowledge-based approach in designing combinatorial or medicinal chemistry libraries,” J. Comb. Chem., Jan. 1999; 1(1): 55–68. doi: 10.1021/cc9800071.
29. D. F. Veber et al., “Molecular properties that influence the oral bioavailability of drug candidates,” J. Med. Chem., Jun. 2002; 45(12): 2615–2623. doi: 10.1021/jm020017n.
30. T. J. Hou et al., “ADME evaluation in drug discovery,” J. Chem. Inf. Comput. Sci., Nov. 2003; 43(6): 2137–2152. doi: 10.1021/ci034184n.
31. J. H. Lin and A. Y. Lu, “Role of pharmacokinetics and metabolism in drug discovery,” Curr. Top. Med. Chem., Jun. 2007; 7(11): 1123–1130. doi: 10.2174/156802607780960519.
32. R. P. Vivek-Ananth et al., “Potential phytochemical inhibitors of SARS-CoV-2 helicase Nsp13: A molecular docking and dynamic simulation study,” Mol. Divers., Feb. 2022; 26(1): 429–442. doi: 10.1007/s11030-021-10251-1.
33. M. P. Y. Goh et al., “The analgesic potential of Litsea species: A systematic review,” Molecules, Apr. 2024; 29(9): 2079. doi: 10.3390/molecules29092079.
34. Q. Peng et al., “Preparation of protein-stabilized Litsea cubeba essential oil nano-emulsion by ultrasonication: Bioactivity, stability, in vitro digestion, and safety evaluation,” Ultrason. Sonochem., Jul. 2024; 107: 106892. doi: 10.1016/j.ultsonch.2024.106892.
35. T. R. Amparo et al., "Brazilian essential oils as a source for the discovery of new anti-COVID-19 drug: A review guided by in silico study," Phytochem. Rev., Oct. 2021; 20(5): 1–20. doi: 10.1007/s11101-021-09754-4.
36. A. H. Arbab et al., “In vitro evaluation of novel antiviral activities of 60 medicinal plant extracts against hepatitis B virus,” Exp. Ther. Med., Jul. 2017; 14(1): 626–634. doi: 10.3892/etm.2017.4530.
37. A. Astani et al., “Comparative study on the antiviral activity of selected monoterpenes derived from essential oils,” Phytother. Res., May 2010; 24(5): 673–679. doi: 10.1002/ptr. 2955.
38. A. Ahmadi et al., “Inhibition of chikungunya virus replication by hesperetin and naringenin,” RSC Adv., Jul. 2016; 6(80): 69421–69430. doi: 10.1039/C6RA16640G.
39. S. Ganesan et al., “Quercetin inhibits rhinovirus replication in vitro and in vivo,” Antiviral Res., Jun. 2012; 94(3): 258–271. doi: 10.1016/j.antiviral.2012.03.005.
40. J. Goldwasser et al., “Naringenin inhibits the assembly and long-term production of infectious hepatitis C virus particles through a PPAR-mediated mechanism,” J. Hepatol., Nov. 2011; 55(5): 963–971. doi: 10.1016/j.jhep.2011.02.011.
41. H. D. Gravina et al., “In vitro assessment of the antiviral potential of trans-cinnamic acid, quercetin and morin against equid herpesvirus 1,” Res. Vet. Sci., Dec. 2011; 91(3): e158-e162. doi: 10.1016/j.rvsc.2010.11.010.
42. J. Guo et al., “Genistein interferes with SDF-1- and HIV-mediated actin dynamics and inhibits HIV infection of resting CD4 T cells,” Retrovirology, Jun. 2013; 10(62). doi: 10.1186/1742-4690-10-62.
43. L. Henss et al., “The green tea catechin epigallocatechin gallate inhibits SARS-CoV-2 infection,” J. Gen. Virol., Apr. 2021; 102(4): 001574. doi: 10.1099/jgv. 0.001574.
44. M. R. Jennings and R. J. Parks, “Curcumin as an antiviral agent,” Viruses, Nov. 2020; 12(11): 1242. doi: 10.3390/v12111242.
45. Z. Y. Jiang et al., “Anti-HBV active constituents from Piper longum,” Bioorg. Med. Chem. Lett., Apr. 2013; 23(7): 2123–2127. doi: 10.1016/j.bmcl.2013.01.118.
46. W. Dai et al., “Structure-based design of antiviral drug candidates targeting the SARS-CoV-2 main protease,” Science, Jun. 2020; 368(6497): 1331–1335. doi: 10.1126/science.abb4489.
47. S. Dallakyan and A. J. Olson, “Small-molecule library screening by docking with PyRx. Chemical Biology. Berlin, Germany: Springer, 2015; 243–250.
48. P. M. Da Silva et al., "Honey: Chemical composition, stability, and authenticity," Food Chem., Apr. 2016; 196: 309–323. doi: 10.1016/j.foodchem.2015.09.051.
49. H. Wang et al., “Structure-based discovery of dual pathway inhibitors for SARS-CoV-2 entry,” Nat. Commun., Nov. 2023; 14: 7574. doi: 10.1038/s41467-023-42526-6.
50. Y. Li et al., “Omicsynin B4 potently blocks coronavirus infection by inhibiting host proteases cathepsin L and TMPRSS2,” Antiviral Res., Jun. 2023; 214: 105606. doi: 10.1016/j.antiviral.2023.105606.